

## Enhancement of Superdeformed Band Population in $^{135}\text{Nd}$

J. M. Nieminen,<sup>1</sup> S. Flibotte,<sup>1</sup> M. Cromaz,<sup>3</sup> A. Galindo-Uribarri,<sup>2</sup> G. Gervais,<sup>1</sup> D. S. Haslip,<sup>1</sup> V. P. Janzen,<sup>2</sup>  
D. C. Radford,<sup>2</sup> C. E. Svensson,<sup>1</sup> J. C. Waddington,<sup>1</sup> D. Ward,<sup>2</sup> and J. N. Wilson<sup>1</sup>

<sup>1</sup>*Department of Physics and Astronomy, McMaster University, Hamilton, Ontario, Canada L8S 4M1*

<sup>2</sup>*AECL, Chalk River Laboratories, Chalk River, Ontario, Canada K0J 1J0*

<sup>3</sup>*Department of Physics, University of Toronto, Toronto, Ontario, Canada M5S 1A7*

(Received 4 December 1996)

It is proposed that the differences in superdeformed band population observed in recent experiments result from a modification of the compound-nucleus angular momentum distribution due to the presence of low-lying vibrational states in the projectile and/or target nuclei. To test this hypothesis the nucleus  $^{135}\text{Nd}$  was studied with the reactions  $^{74}\text{Ge} + ^{64}\text{Ni}$  and  $^{26}\text{Mg} + ^{112}\text{Cd}$ . The  $^{74}\text{Ge}$ -induced reaction was found to preferentially populate high-spin states, including superdeformed states. Statistical-model calculations are consistent with the present observations provided coupled-channel effects are taken into account. [S0031-9007(97)03150-5]

PACS numbers: 21.10.Re, 25.70.Gh, 25.70.Jj, 27.60.+j

It has been observed that, in contrast to superdeformed rotational bands in nuclei with mass  $A \sim 130$  [1,2] and  $A \sim 190$  [3,4], the population of superdeformed bands in the  $A \sim 150$  mass region is enhanced for mass-symmetric fusion-evaporation reactions [5,6]. The reason for this enhancement is not yet understood. Smith *et al.* [5] suggested that it is an entrance-channel effect associated with an increase of the fusion time for mass-symmetric reactions as compared to mass-asymmetric reactions. However, a recent study reported no entrance-channel effects in the  $\gamma$ -ray decay of giant dipole resonances (GDR) in the compound nucleus  $^{146}\text{Gd}$  [7], even though GDR are very sensitive to the above-mentioned time delay. Furthermore, according to dissipative collision calculations [2,7], the time required to reach equilibrium does not depend on the asymmetry of the reaction used in the  $A \sim 150$  mass region. This suggests that the feeding enhancement of superdeformed bands is not an entrance-channel effect associated with increased fusion time for mass-symmetric reactions. Therefore, alternative explanations should be investigated.

The possible existence of entrance-channel effects in the decay of a compound nucleus has been investigated in the past. For example, Kühn *et al.* [8] measured neutron spectra and neutron multiplicity distributions for the nearly mass-symmetric reaction  $^{64}\text{Ni} + ^{92}\text{Zr}$  and found that statistical-model calculations overestimated the multiplicity. It was suggested that this was due to trapping in a superdeformed minimum and that the neutron multiplicity for a given spin interval should depend on the mass asymmetry of the entrance channel. A later study by Janssens *et al.* [9] reported agreement between statistical-model calculations and experimental observations of neutron multiplicities for the mass-asymmetric reaction  $^{12}\text{C} + ^{144}\text{Sm}$  but not for the mass-symmetric reaction  $^{64}\text{Ni} + ^{92}\text{Zr}$ . With these same reactions, Ruckelshausen *et al.* [10] measured the ratio

of  $2n$  to  $3n$  cross sections as a function of compound-nucleus spin and noted fewer evaporated neutrons in the  $^{64}\text{Ni}$ -induced reaction. The interpretation of the results for the latter two studies followed that given by Kühn *et al.* [8].

The realization that fusion-barrier fluctuations [11] broaden the compound-nucleus spin distribution [12–14], thus resulting in an increase of the rotational energy and a reduction in effective temperature, provided an alternative explanation for the reduction of the neutron-evaporation probability noted to occur in mass-symmetric reactions. Haas *et al.* [15] measured cross sections and  $\gamma$ -ray multiplicities for neutron evaporation channels in mass-symmetric and mass-asymmetric near-barrier reactions. It was concluded that nuclear shape vibrations were necessary to explain measured  $\gamma$ -ray multiplicities of individual exit channels for more mass-symmetric reactions and that, near the barrier, the average angular momentum transferred greatly depends on the asymmetry of the entrance channel. With calculations that incorporated coupling to inelastic channels, Love *et al.* [16] were able to explain the observed neutron multiplicity for the reaction  $^{64}\text{Ni} + ^{92}\text{Zr}$ , and by studying the feeding pattern of collective states concluded that trapping in superdeformed states at low spin did not occur.

In a recent study, Barreto *et al.* [17] readdressed the inconsistencies between the two interpretations in a study dealing with the decay of  $^{164}\text{Yb}^*$  formed in the reactions  $^{16}\text{O} + ^{148}\text{Sm}$  and  $^{64}\text{Ni} + ^{100}\text{Mo}$ . Gamma-ray fold distributions of the various evaporation channels showed differences depending on the entrance channel. The results were consistent with fusion models that predict an increase in the width of the compound-nucleus spin distribution in the  $^{64}\text{Ni}$ -induced reaction, thus agreeing with a shape-vibration explanation.

The present work attempts to take this idea one step further by studying the relationship between the enhancement

of superdeformed band population and modification of the compound-nucleus spin distribution due to the presence of low-lying vibrational states in the projectile and/or target nuclei. The so-called entrance-channel effects observed in the  $A \sim 150$  mass region could possibly be explained by this phenomenon. However, in order to properly study coupled-channel effects, a matching of the classical angular momentum,  $l_{\max}$  [18], and the excitation energy,  $E^*$ , is essential for any two reactions being compared. In the  $A \sim 150$  mass region, such a matching occurs at angular momenta where fission of the compound nucleus competes with particle evaporation and a study of spin distributions becomes difficult. Superdeformed bands in the  $A \sim 130$  mass region can, however, be populated at relatively low spins without competition with the fission process. For this reason, in a first study, it is more convenient to search for coupled-channel effects in the  $A \sim 130$  mass region.

Reactions ideally suited for this particular study were  $^{74}\text{Ge} + ^{64}\text{Ni}$  at 239 MeV ( $E^* = 50.5$  MeV at midtarget) and  $^{26}\text{Mg} + ^{112}\text{Cd}$  at 94 MeV ( $E^* = 50.7$  MeV at midtarget), where the nucleus  $^{135}\text{Nd}$  [19] is populated through the  $3n$  exit channel. The  $^{74}\text{Ge}$  and  $^{26}\text{Mg}$  beams were provided by the Tandem Accelerator Superconducting Cyclotron (TASCC) facility at the Chalk River Laboratories. The  $^{64}\text{Ni}$  and  $^{112}\text{Cd}$  targets consisted of thin foils of  $\sim 380$  and  $\sim 500 \mu\text{g}/\text{cm}^2$ , respectively. Gamma rays emitted by the deexciting nuclei were detected with the  $8\pi$  Spectrometer [20,21] which comprises 20 Compton-suppressed HPGe detectors and a 71-element bismuth germanate (BGO) ball used as a  $\gamma$ -ray calorimeter and multiplicity detector. In order for an event to be recorded on tape, two or more HPGe detectors and two or more BGO elements had to fire in prompt time coincidence. The number of  $\gamma$ - $\gamma$  coincidences collected for the  $^{74}\text{Ge} + ^{64}\text{Ni}$  and  $^{26}\text{Mg} + ^{112}\text{Cd}$  reactions totaled  $19 \times 10^6$  and  $11 \times 10^6$ , respectively.

Shown in Fig. 1 are theoretical fusion cross sections as functions of the compound-nucleus spin calculated with the code CCFUS [22]. The accepted deformation parameters,  $\beta_\lambda$ , for the first  $2^+$  and  $3^-$  excited states of  $^{74}\text{Ge}$ ,  $^{64}\text{Ni}$ ,  $^{26}\text{Mg}$ , and  $^{112}\text{Cd}$  (see Table I) were used as inputs to CCFUS. Target thicknesses were taken into account for all calculations by integrating over the appropriate energy spreads. The upper panel of Fig. 1 presents the cross sections when no coupling to low-lying vibrational states is included in the calculations, illustrating the closely matched spin distributions. Having similar uncoupled spin distributions is essential for the present investigation. The lower panel gives the cross sections when coupled channels are taken into account, showing a  $10\hbar$  increase in spin for the  $^{74}\text{Ge}$ -induced reaction.

Shown in Fig. 2 are the  $K$  distributions, where  $K$  is the number of BGO elements that fired, for the two reactions studied and for exit channels leading to the residual nuclei  $^{134}\text{Nd}$ ,  $^{135}\text{Nd}$ , and  $^{136}\text{Nd}$ . For comparison, the  $K$  distribution for superdeformed states in  $^{135}\text{Nd}$  is also

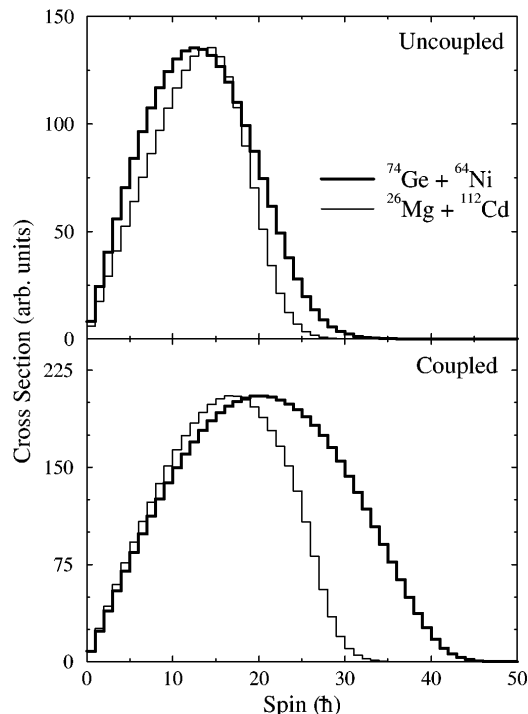


FIG. 1. Calculated compound-nucleus spin distributions. Upper panel: spin distributions when no coupling to low-lying vibrational states is included in the calculations. Lower panel: spin distributions when coupled channels are taken into consideration. Target thicknesses were taken into account in the calculations and the curves were normalized at their maxima for each panel.

shown. A large centroid shift between the two reactions is evident for the  $2n$  channel and becomes less apparent when the neutron multiplicity increases; this feature has been noted in earlier studies [10,15,17]. It should also be pointed out that similar centroid shifts have been reported for other superdeformed bands [2,4].

To gain an understanding of coupled-channel effects at high spin, nuclei exhibiting discrete superdeformed states may be studied. Shown in Fig. 3 are background-subtracted coincidence spectra for the superdeformed band in  $^{135}\text{Nd}$ , for the two reactions, obtained by summing clean coincidences. As predicted by coupled-channel calculations, the superdeformed band is seen to higher spin in the  $^{74}\text{Ge}$ -induced reaction than in the  $^{26}\text{Mg}$ -induced reaction. More precisely, the band is seen up to the 1147 keV  $32.5\hbar \rightarrow 30.5\hbar$  transition for the former

TABLE I. Energies and deformation parameters for the first  $2^+$  and  $3^-$  excited states.

Nucleus	$\beta_2$ : Energy (MeV)	$\beta_3$ : Energy (MeV)
$^{74}\text{Ge}$	0.29 : 0.60	0.16 : 2.54
$^{64}\text{Ni}$	0.22 : 1.34	0.23 : 3.56
$^{26}\text{Mg}$	0.48 : 1.81	0.18 : 6.88
$^{112}\text{Cd}$	1.18 : 0.62	0.17 : 2.01

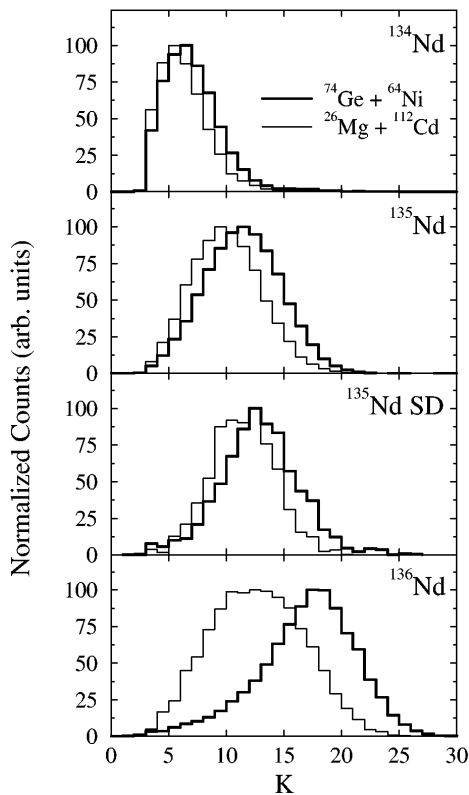


FIG. 2. Total number of firing BGO elements,  $K$ , measured for the two reactions. Shown are the  $K$  distributions corresponding to transitions between normally deformed states in  $^{134}\text{Nd}$ ,  $^{135}\text{Nd}$ , and  $^{136}\text{Nd}$ , and for superdeformed states in  $^{135}\text{Nd}$ .

reaction, whereas the last discernible transition for the latter reaction is 1011 keV  $28.5\hbar \rightarrow 26.5\hbar$ .

The ratio of the intensity of a given  $\gamma$ -ray transition measured for the  $^{26}\text{Mg}$ -induced reaction to the intensity of that same transition measured for the  $^{74}\text{Ge}$ -induced reaction was determined as a function of spin and is shown in Fig. 4. The intensities of the lowest spins measured, for the various exit channels, have been normalized to unity for both reactions. To illustrate the dramatic difference in the population of high-spin states between the two reactions one can consider the results for the superdeformed band. At spin  $16.5\hbar$ , for example, the population intensity of the superdeformed band in  $^{135}\text{Nd}$  measured with the  $^{74}\text{Ge}$ -induced reaction is enhanced by  $\sim 2$  times relative to the corresponding intensity observed in  $^{26}\text{Mg}$ -induced reaction. At spin  $26.5\hbar$  the enhancement is considerably larger having a value of  $\sim 20$ .

The theoretical spin distributions, shown in Fig. 1, were used as inputs to the statistical code EVAP [23]. With the level density formalism of Gilbert and Cameron [24] and a level density parameter of  $a = A/9.0 \text{ MeV}^{-1}$ , cross sections of various exit channels were calculated and compared to values extracted from experiment (see Table II). It is clear that the inclusion of coupled channels is necessary. Two different level density parameters are usually used in statistical codes when modeling the population

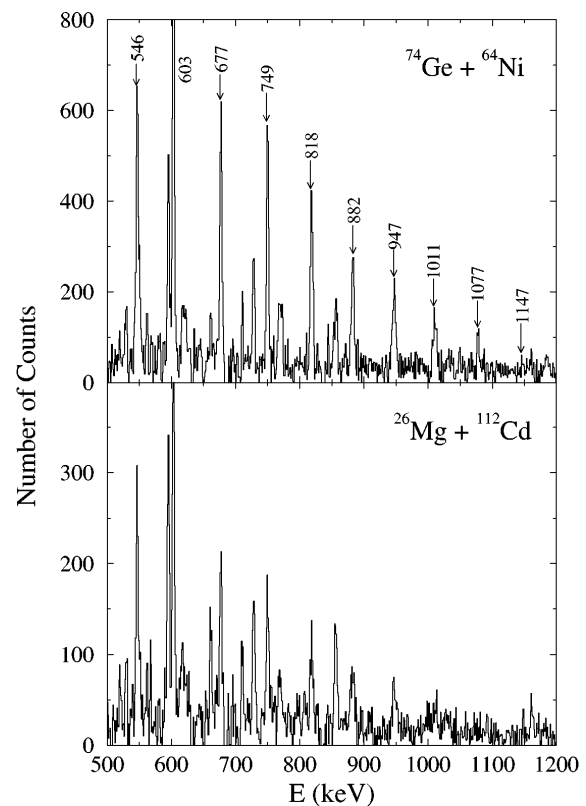


FIG. 3. Partial coincidence spectra for the superdeformed band in  $^{135}\text{Nd}$  for the two reactions studied. In both cases the spectra were obtained by summing coincidences of the 546, 677, 749, 818, 882, 947, 1011, 1077, and 1147 keV lines.

of normal and superdeformed states (see, for example, [25,26]). This level density difference is however known to mainly influence the statistical spectra and most likely does not affect the enhancement of interest here. With

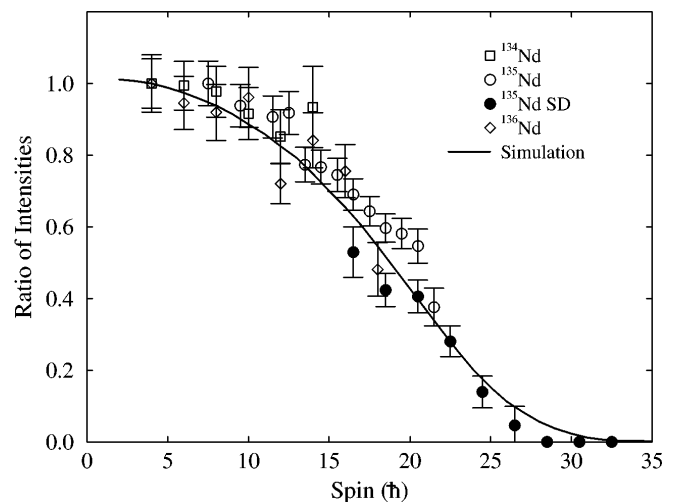


FIG. 4. The ratio of intensities ( $^{26}\text{Mg}$ -induced reaction/ $^{74}\text{Ge}$ -induced reaction: see text for details) as a function of spin; where spin refers to the initial state of a given  $\gamma$  ray. The smooth solid line is a theoretical simulation done with the code EVAP. The coupled spin distributions calculated with CCFUS were used as input to the statistical code.

TABLE II. Measured and calculated relative cross sections (C.S.) for the various channels observed. Note that the cross section for the  $3n$  channel has been normalized to unity. All experimental uncertainties are within one percent of the stated relative cross section.

Reaction	Residual nucleus	Exp. C.S.	Calc. C.S. (uncoupled)	Calc. C.S. (coupled)
$^{74}\text{Ge} + ^{64}\text{Ni}$	$^{135}\text{Nd}$	1.00	1.00	1.00
	$^{136}\text{Nd}$	0.45	0.13	0.45
	$^{134}\text{Nd}$	0.08	0.21	0.11
	$^{132}\text{Ce}$	0.11	0.18	0.17
$^{26}\text{Mg} + ^{112}\text{Cd}$	$^{135}\text{Nd}$	1.00	1.00	1.00
	$^{136}\text{Nd}$	0.25	0.10	0.17
	$^{134}\text{Nd}$	0.09	0.21	0.15
	$^{132}\text{Ce}$	0.12	0.17	0.16

the coupled spin distribution as input to EVAP, the theoretical enhancement was calculated. This is represented as the solid curve (normalized to unity at spin 4) in Fig. 4. The agreement between theory and experiment is excellent. However, it should be pointed out that the code CCFUS is a relatively simple approach to the coupled-channel problem and more refined calculations should probably be performed for the systems investigated in the present work. It is interesting to note that the theoretical enhancement compares equally well to the trend seen for superdeformed states in  $^{135}\text{Nd}$  as it does to the trend seen for normally deformed states. This is an indication that the trend in the enhancement is purely a spin effect and that trapping in a superdeformed minimum probably does not occur.

To summarize, enhancement of superdeformed band population in  $^{135}\text{Nd}$  has been observed for the reaction  $^{74}\text{Ge} + ^{64}\text{Ni}$  at 239 MeV compared to the reaction  $^{24}\text{Mg} + ^{112}\text{Cd}$  at 94 MeV. This is the first report of such an effect in the  $A \sim 130$  mass region and the first time that such an enhancement has been measured as a function of spin for a superdeformed band. The results are consistent with coupled-channel calculations that predict a broadening of the compound-nucleus spin distribution for the  $^{74}\text{Ge}$ -induced reaction. A similar explanation may be applicable to the enhancement observed for superdeformed states in the  $A \sim 150$  mass region. However, the situation is more complex in the  $A \sim 150$  mass region due to the competition between fission and particle evaporation at high spin and more experimental work is needed. In particular, it would be important to obtain reliable feeding patterns of superdeformed bands for the reactions where population enhancements have been observed. Such studies can only be done with  $\gamma$ -ray spectrometers of the third generation like GAMMASPHERE, EUROGAM, and GASP.

This work has been partially funded by the Natural Sciences and Engineering Research Council of Canada (NSERC) and Atomic Energy of Canada Limited (AECL). We thank the staff at TASCC for supplying the beams.

- [1] S.M. Mullins, J. Nyberg, A. Maj, M.S. Metcalfe, P.J. Nolan, P.H. Regan, R. Wadsworth, and R.A. Wyss, *Phys. Lett. B* **312**, 272 (1993).
- [2] G. Viesti *et al.*, *Nucl. Phys.* **A579**, 225 (1994).
- [3] T. Lauritsen *et al.*, in Proceedings of the International Conference on Nuclear Structure at High Angular Momentum, Ottawa (unpublished) p. 59; Report No. AECL-10613, 1992.
- [4] F. Soramel *et al.*, *Phys. Lett. B* **350**, 173 (1995).
- [5] G. Smith *et al.*, *Phys. Rev. Lett.* **68**, 158 (1992).
- [6] S. Flibotte *et al.*, *Phys. Rev. C* **45**, R889 (1992).
- [7] S. Flibotte *et al.*, *Phys. Rev. C* **53**, R533 (1996).
- [8] W. Kühn, P. Chowdhury, R. V.F. Janssens, T.L. Khoo, F. Haas, J. Kasagi, and R.M. Ronningen, *Phys. Rev. Lett.* **51**, 1858 (1983).
- [9] R. V.F. Janssens *et al.*, *Phys. Lett. B* **181**, 16 (1986).
- [10] A. Ruckelshausen *et al.*, *Phys. Rev. Lett.* **56**, 2356 (1986).
- [11] N. Rowley, G.R. Satchler, and P.H. Stelson, *Phys. Lett. B* **254**, 25 (1991).
- [12] S. Landowne and C.H. Dasso, *Phys. Lett.* **138B**, 32 (1984).
- [13] R. Vandebosch, *Annu. Rev. Nucl. Part. Sci.* **42**, 447 (1992).
- [14] W. Reisdorf, *J. Phys. G* **20**, 1297 (1994), and references therein.
- [15] B. Haas *et al.*, *Phys. Rev. Lett.* **54**, 398 (1985).
- [16] D.J.G. Love, P.J. Bishop, A. Kirwan, P.J. Nolan, D.J. Thornley, A.H. Nelson, and P.J. Twin, *Phys. Rev. Lett.* **57**, 551 (1986).
- [17] J.L. Barreto *et al.*, *Phys. Rev. C* **48**, 2881 (1993).
- [18] R. Bass, *Phys. Lett.* **47B**, 139 (1973).
- [19] M.A. Deleplanque *et al.*, *Phys. Rev. C* **52**, R2302 (1995).
- [20] H.R. Andrews *et al.*, Report No. AECL-8329, 1984.
- [21] J.P. Martin *et al.*, *Nucl. Instrum. Methods Phys. Res., Sect. A* **257**, 301 (1987).
- [22] C.H. Dasso and S. Landowne, *Comput. Phys. Commun.* **46**, 187 (1987).
- [23] Computer code EVAP, by N.G. Nicolis, D.G. Sarantites, and J.R. Beene (unpublished).
- [24] A. Gilbert and A.G.W. Cameron, *Can. J. Phys.* **43**, 1446 (1965).
- [25] K. Schiffer, B. Herskind, and J. Gascon, *Z. Phys. A* **332**, 17 (1989).
- [26] T.L. Khoo *et al.*, *Nucl. Phys.* **A557**, 83c (1993).